

Linear response in the uniformly heated granular gas

Bernardo Sánchez-Rey

Departamento de Física Aplicada I, E.P.S., Universidad de Sevilla, Virgen de África 7, E-41011 Sevilla, Spain

Antonio Prados

Física Teórica, Universidad de Sevilla, Apartado de Correos 1065, E-41080 Sevilla, Spain

(Dated: October 21, 2020)

We analyse the linear response properties of the uniformly heated granular gas, for which the stationary value of the granular temperature is fixed by the intensity of the stochastic driving. We focus on the time evolution of the granular temperature in two specific situations. First, we look into its response to a small change of the driving intensity. Second, we investigate its behaviour in a more complex experiment, specifically a Kovacs-like protocol. The analytical results are compared with numerical simulations of the kinetic equation, and a good agreement is found.

I. INTRODUCTION

Linear response is at the root of many important results in physics. In this respect, the fluctuation-dissipation theorem is a milestone in the development of (non-equilibrium) statistical physics [1–3]. In its original form, it relates the linear relaxation of a system to equilibrium, from an initial non-equilibrium state, with certain equilibrium time correlation functions. Very recently, this result has been extended to more general situations, which include the relaxation to non-equilibrium steady states (NESS) [4].

The above general picture makes it relevant to investigate the linear relaxation of intrinsically out-of-equilibrium systems, such as granular gases [5–8], to their NESS. Due to the energy dissipation in collisions, an external energy input mechanism is needed to drive the system to a NESS. One of the simplest physical situations is that of the uniformly heated granular gas, in which all the particles of the gas are submitted to independent white noise forces of a given amplitude [9, 10]. Therein, the granular gas remains homogeneous for all times, if it was initially so, and the main physical property of the granular gas is the granular temperature—basically, the average kinetic energy per degree of freedom. It is the amplitude of the white noise force, i.e. the intensity of this *stochastic thermostat*, that determines the stationary value of the granular temperature.

The main purpose of this work is to analyse the linear relaxation of the granular temperature in the uniformly heated granular gas, in several different physical situations. Due to the non-Gaussian character of the velocity distribution function, the velocity moments obey an infinite hierarchy of coupled ordinary differential equations (ODE), which must be supplemented with a closure assumption. Here, we work in the first Sonine approximation [10, 11], in which the state of the granular system is characterised by the granular temperature T and the second Sonine coefficient a_2 —the excess kurtosis. The dynamics of the gas is described by a set of two ODEs for the temperature and the excess kurtosis, which are non-linear and have been shown to describe accurately

the granular gas in many different physical situations, see for example [9, 10, 12–14].

First, we would like to investigate the response of the gas to an instantaneous perturbation of the driving intensity. For small enough perturbations, the evolution equations can be linearised and thus analytically solved. This analytical prediction is compared with the Direct Simulation Monte Carlo (DSMC) numerical integration of the kinetic equation. Specifically, we are interested in the relaxation behaviour of the granular temperature in this single-jump experiment: whether it is exponential or not, its dependence on the non-elasticity of the system, etc. For example, non-exponential relaxation [15–21] is a key ingredient for the emergence of aging and memory effects [22–33], such as the Kovacs effect described below.

More detailed insight into the dynamics of the system can be acquired with more complicated driving protocols. A particularly relevant one is the so-called Kovacs experiment [34–36], in which the system is submitted to a protocol that involves two jumps of the driving. Thereby, it is prepared in a state such that the value of the “thermodynamic” property of interest equals its steady state value. If the subsequent behaviour is non-monotonic, with the property departing from its steady value before returning thereto, additional variables are needed to completely characterise the steady state of the system. This non-monotonic behaviour has been termed the Kovacs effect.

The Kovacs effect has been extensively analysed in the realm of glassy systems [36–46]. These studies have been mainly done in the non-linear regime, although there are some exact general results for molecular systems—such that the steady distribution is the canonical one—with Markovian dynamics in linear response theory [36]. Interestingly, some of these linear response results have been extended to athermal systems—for which the state reached for long times is a NESS—quite recently, both for discrete time and continuous time dynamics [47, 48].

The available results in linear response can be summarised as follows. For both molecular and athermal systems, i.e. regardless of the specific shape of the stationary distribution, the Kovacs hump can be written in terms of the relaxation functions for the direct, single-jump, re-

laxation experiment [36, 47, 48]. This structure makes it possible to give some general properties of the hump for molecular systems, because the direct relaxation function of the macroscopic variable is a sum of decreasing exponential modes with all the coefficients being positive—as a consequence of the fluctuation-dissipation relation [3]. In particular, it can be ensured that the Kovacs hump cannot change sign, has only one extremum, and—with its usual definition—the latter is always a maximum [36].

For athermal systems, the situation is different from the one just described above. Assuming that the NESS is linearly stable, the direct linear relaxation function is a sum of decreasing exponential modes. Notwithstanding, the coefficients do not need to be necessarily positive and this opens the door to the emergence of *anomalous* behaviour: even when only one extremum is present, the sign of the Kovacs hump may change with the system parameters. Thus, both a maximum (normal behaviour) and a minimum (anomalous) can be observed. Moreover, more complex responses, for instance with multiple extrema, cannot be ruled out.

The above picture is consistent with recent observations in granular fluids. In the smooth granular gas, both *normal* and *anomalous* behaviour have been reported, with the latter coming about for large enough inelasticity [13, 49]. In the rough case, there appear large humps and complex responses with more than one extremum [50]. It must be stressed that these observations correspond to the non-linear regime, for large jumps of the driving. Therefore, it seems worth elucidating the fate of these behaviours in the linear response limit.

The organisation of the paper is as follows. In Sec. II, we put forward the evolution equations for the granular temperature and the excess kurtosis and carry out their linearisation around the NESS in Sec. II A. The linear relaxation of the granular temperature to an instantaneous change of the driving is considered in Sec. III, for different values of the inelasticity. Next, Sec. IV is devoted to the analysis of the Kovacs experiment. Finally, conclusions and a brief discussion of perspectives for future work are presented in Sec. V.

II. EVOLUTION EQUATIONS

Let us analyse the dynamics of a granular gas of smooth hard spheres [7]. This system comprises N hard particles of mass m and diameter σ in dimension d , which undergo inelastic collisions. In the binary collisions, the tangential component of the relative velocity remains unaltered while the normal component is reversed and shrunk by a factor α , the normal restitution coefficient, $0 \leq \alpha \leq 1$. Apart from the elastic limit $\alpha = 1$, kinetic energy is lost in every collision and the undriven system “cools”, in the sense that its granular temperature—basically the average of the kinetic energy—decreases monotonically in time.

We consider the uniformly heated granular gas, i.e.

the system described above is also submitted to a random forcing that inputs energy into the system. This is modelled as independent white noise forces $\mathbf{F}_i^{(p)}(t)$ acting over each grain, $\langle F_i^{(p)}(t) \rangle = 0$ and $\langle F_i^{(p)}(t) F_j^{(q)}(t') \rangle = m^2 \xi^2 \delta_{ij} \delta_{pq} \delta(t - t')$, $i, j = 1, \dots, d$, $p, q = 1, \dots, N$. As a consequence, the system reaches a steady state in the long time limit, in which the energy input by the thermostat cancels—in average—the energy loss in collisions [9].

At the kinetic level of description, the dynamical evolution of the system is governed by the Boltzmann-Fokker-Planck equation for the velocity distribution function [9, 10]. Being the granular gas an intrinsically non-equilibrium system, its velocity distribution function is non-Gaussian, even in the steady state. The granular temperature $T(t)$ is defined as

$$\frac{d}{2} T(t) \equiv \left\langle \frac{1}{2} m v^2(t) \right\rangle. \quad (1)$$

To measure the departure from the Maxwellian distribution, the simplest approach is to consider the excess kurtosis a_2 ,

$$a_2 = \frac{d}{d+2} \frac{\langle v^4 \rangle}{\langle v^2 \rangle^2} - 1, \quad (2)$$

which vanishes for the Gaussian case. In kinetic theory, working with the pair (T, a_2) is known as the first Sonine approximation, because a_2 is the first non-zero coefficient of the expansion of the velocity distribution function in a series of Sonine polynomials [9, 11].

The evolution equations for the granular temperature and the excess kurtosis are derived from the Boltzmann-Fokker-Planck equation [9, 11–13]. They are usually written in terms of the stationary values of the granular temperature and the excess kurtosis,

$$T_s = \left[\frac{m \xi^2}{\zeta_0 \left(1 + \frac{3}{16} a_2^s\right)} \right]^{2/3}, \quad \zeta_0 = \frac{2n\sigma^{d-1} (1 - \alpha^2) \pi^{\frac{d-1}{2}}}{\sqrt{m} d \Gamma(d/2)}, \quad (3a)$$

$$a_2^s = \frac{16(1 - \alpha)(1 - 2\alpha^2)}{73 + 56d - 24d\alpha - 105\alpha + 30(1 - \alpha)\alpha^2}. \quad (3b)$$

By defining scaled—order of unity—variables as follows,

$$\theta = \frac{T}{T_s}, \quad A_2 = \frac{a_2}{a_2^s}, \quad \tau = \frac{\zeta_0 \sqrt{T_s}}{2} t. \quad (4)$$

the evolution equations are

$$\frac{d\theta}{d\tau} = 2 \left[1 - \theta^{3/2} + \frac{3}{16} a_2^s \left(1 - A_2 \theta^{3/2} \right) \right], \quad (5a)$$

$$\theta \frac{dA_2}{d\tau} = 4 \left[\left(\theta^{3/2} - 1 \right) A_2 + B \theta^{3/2} (1 - A_2) \right], \quad (5b)$$

with the parameter B given by [51]

$$B = \frac{73 + 8d(7 - 3\alpha) + 15\alpha[2\alpha(1 - \alpha) - 7]}{16(1 - \alpha)(3 + 2d + 2\alpha^2)}. \quad (6)$$

A couple of comments on the evolution equations (5) are appropriate. First, they are non-linear, so in general it is not possible to write down an analytical closed solution for them [52]. Second, the parameters B and a_2^s only depend on α and d , being independent of the steady value of the temperature. In fact, all the dependence on T_s has been incorporated into the time scale τ introduced in Eq. (4).

A. Linearisation around the steady state

In this paper, we are interested in the linear relaxation of the granular gas to the steady state, in which the temperature and the excess kurtosis are $\theta_s = 1$ and $A_2^s = 1$, as a consequence of the scaling. Therefore, we write

$$\theta = 1 + \delta\theta, \quad A_2 = 1 + \delta A_2, \quad (7)$$

insert them into Eq. (5) and neglect nonlinearities. The following linear system is thus obtained,

$$\frac{d}{dt}\delta\mathbf{z} = \mathbf{M} \cdot \delta\mathbf{z}, \quad (8a)$$

$$\delta\mathbf{z} \equiv \begin{pmatrix} \delta\theta \\ \delta A_2 \end{pmatrix}, \quad \mathbf{M} \equiv \begin{pmatrix} -3\left(1 + \frac{3}{16}a_2^s\right) & -\frac{3}{8}a_2^s \\ 6 & -4B \end{pmatrix}. \quad (8b)$$

The matrix—or operator [53]— \mathbf{M} does not depend on the noise intensity ξ but only on the restitution coefficient α and the dimension d . This is a consequence of the rhs of the non-linear system (5) being independent of T_s , as already pointed out above.

In the following, we denote the elements of the matrix \mathbf{M} by M_{ij} , i.e.

$$\begin{aligned} M_{11} &= -3\left(1 + \frac{3}{16}a_2^s\right), & M_{12} &= -\frac{3}{8}a_2^s, \\ M_{21} &= 6, & M_{22} &= -4B. \end{aligned} \quad (9)$$

The eigenvalues of the matrix \mathbf{M} are both negative,

$$\lambda_{\pm} = \frac{\text{Tr } \mathbf{M} \pm \sqrt{(\text{Tr } \mathbf{M})^2 - 4 \det \mathbf{M}}}{2} < 0, \quad (10)$$

and the corresponding eigenvectors read

$$\zeta_+ = \begin{pmatrix} M_{12} \\ \lambda_+ - M_{11} \end{pmatrix}, \quad \zeta_- = \begin{pmatrix} M_{12} \\ \lambda_- - M_{11} \end{pmatrix}. \quad (11)$$

The explicit expression for the trace and the determinant of \mathbf{M} are

$$\text{Tr } \mathbf{M} = -4B - 3\left(1 + \frac{3}{16}a_2^s\right) < 0, \quad (12a)$$

$$\det \mathbf{M} = 12B\left(1 + \frac{3}{16}a_2^s\right) + \frac{9}{4}a_2^s > 0. \quad (12b)$$

The general solution of the linear system is

$$\delta\mathbf{z}(\tau) = c_+\zeta_+e^{\lambda_+\tau} + c_-\zeta_-e^{\lambda_-\tau}, \quad (13)$$

or, equivalently,

$$\begin{pmatrix} \delta\theta(\tau) \\ \delta A_2(\tau) \end{pmatrix} = c_+\begin{pmatrix} M_{12} \\ \lambda_+ - M_{11} \end{pmatrix}e^{\lambda_+\tau} + c_-\begin{pmatrix} M_{12} \\ \lambda_- - M_{11} \end{pmatrix}e^{\lambda_-\tau}. \quad (14)$$

The constants c_+ and c_- are determined by the initial conditions through the relation

$$\begin{pmatrix} \delta\theta(0) \\ \delta A_2(0) \end{pmatrix} = \delta\mathbf{z}(0) = c_+\zeta_+ + c_-\zeta_-. \quad (15)$$

III. DIRECT RELAXATION AFTER A SINGLE JUMP IN THE DRIVING

Let us consider an experiment in which the system is initially at the steady state corresponding to some value of the driving $\xi + \delta\xi$. At the initial time, the intensity of the driving is suddenly changed from $\xi + \delta\xi$ to ξ : subsequently, the granular gas relaxes from its non-equilibrium steady state (NESS) at $\xi + \delta\xi$ to the corresponding NESS at ξ .

The initial values of the scaled variables are

$$\delta\theta(0) \neq 0, \quad \delta A_2(0) = 0, \quad (16)$$

because the steady value of the temperature depends on the driving intensity but that of the excess kurtosis does not. Eq. (15) predicts that both c_+ and c_- are proportional to $\delta\theta(0)$ in this case, so we write

$$c_{\pm} = \delta\theta(0) \tilde{c}_{\pm} \quad (17)$$

and readily obtain

$$\tilde{c}_+ = \frac{M_{11} - \lambda_-}{M_{12}(\lambda_+ - \lambda_-)}, \quad \tilde{c}_- = \frac{\lambda_+ - M_{11}}{M_{12}(\lambda_+ - \lambda_-)}. \quad (18)$$

Let us introduce a normalised response function for this single-jump experiment. Specifically, we define

$$\phi^{(1)}(\tau) \equiv \frac{\delta\theta(\tau)}{\delta\theta(0)} = \tilde{c}_+\zeta_+e^{\lambda_+\tau} + \tilde{c}_-\zeta_-e^{\lambda_-\tau}. \quad (19)$$

The superindex (1) refers to the first variable, i.e. the scaled granular temperature θ , being the perturbed one at the initial time, as expressed by Eq. (16). In the following, we focus on the relaxation of the granular temperature,

$$\phi_1^{(1)}(\tau) = \frac{\delta\theta(\tau)}{\delta\theta(0)} = a_+e^{\lambda_+\tau} + a_-e^{\lambda_-\tau}, \quad (20)$$

with

$$a_+ = \frac{M_{11} - \lambda_-}{\lambda_+ - \lambda_-}, \quad a_- = \frac{\lambda_+ - M_{11}}{\lambda_+ - \lambda_-}. \quad (21)$$

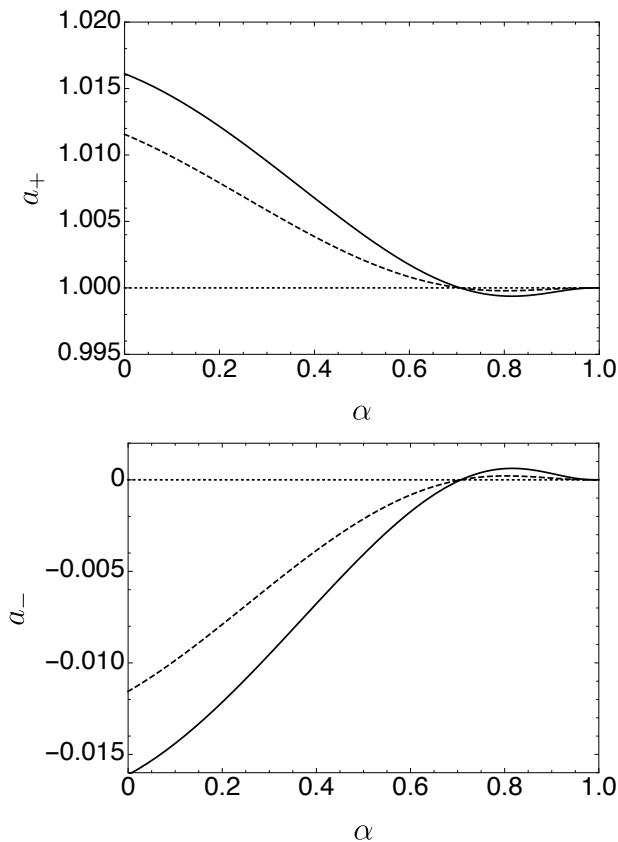


FIG. 1. Coefficients a_{\pm} as a function of the restitution coefficient α . Both the three-dimensional (solid line) and the two-dimensional (dashed line) are plotted. The coefficient a_+ is always positive, whereas a_- changes sign at $\alpha = \alpha_c$ —as given by Eq. (22). Note that $|a_-|$ is quite small throughout, with its least small value at $\alpha = 0$.

In Fig. 1, we show the two coefficients a_+ and a_- as a function of the restitution coefficient α , for $d = 2$ and $d = 3$. Both for the two and the three-dimensional case, two distinct properties are observed: (i) while $a_+ > 0$ for all values of α , a_- changes sign at $\alpha = 1/\sqrt{2}$, specifically

$$\text{sgn}(a_-) = \text{sgn}(\alpha - \alpha_c), \quad \alpha_c = 1/\sqrt{2}, \quad (22)$$

and (ii) the ratio $|a_-/a_+| \ll 1$ for all values of α , with its larger value taking place at $\alpha = 0$, for which it equals 0.0159 (0.0114) for $d = 2$ ($d = 3$). In principle, the change of sign of a_- at α_c might bring about a non-monotonic behaviour of the relaxation function, but this is not the case. In the long time limit, the relaxation is dominated by the largest eigenvalue λ_+ and, therefore,

$$\phi_1^{(1)}(\tau) \sim a_+ e^{\lambda_+ \tau} > 0, \quad (\lambda_+ - \lambda_-)\tau \gg 1. \quad (23)$$

In order to understand the above behaviour of a_{\pm} , we bring to bear the smallness of a_2^s and expand all quantities in powers of a_2^s . In particular, the eigenvalues λ_{\pm}

are given by

$$\lambda_+ = -3 - \frac{9(1+4B)}{16(4B-3)} a_2^s + O(a_2^s)^2, \quad (24)$$

$$\lambda_- = -4B + \frac{9}{4(4B-3)} a_2^s + O(a_2^s)^2. \quad (25)$$

Note that $4B - 3 > 0$ ($\lambda_+ > \lambda_-$). In turn, the corresponding expansion for the coefficients a_{\pm} is

$$a_+ = 1 + \frac{9}{4(4B-3)^2} a_2^s + O(a_2^s)^2, \quad (26)$$

$$a_- = -\frac{9}{4(4B-3)^2} a_2^s + O(a_2^s)^2. \quad (27)$$

On the one hand, it is neatly observed that a_- is proportional to a_2^s , thus being rather small across the whole range of inelasticities. Moreover, the change of sign of a_- at α_c is clearly linked to the vanishing of a_2^s thereat. On the other hand, $a_+ = 1 + O(a_2^s)$ is very close to unity throughout, consistently with the normalisation condition $a_+ + a_- = 1$.

Now we compare our analytical prediction for the relaxation function with numerical data obtained from the DSMC numerical integration of the Boltzmann-Fokker-Planck equation. We have employed a system of $N = 10^6$ hard discs ($d = 2$) of unit mass $m = 1$ and unit diameter $\sigma = 1$, with the binary collision rule between particles i and j

$$\mathbf{v}'_i = \mathbf{v}_i - \frac{1+\alpha}{2} (\hat{\boldsymbol{\sigma}} \cdot \mathbf{v}_{ij}) \hat{\boldsymbol{\sigma}}, \quad \mathbf{v}'_j = \mathbf{v}_j + \frac{1+\alpha}{2} (\hat{\boldsymbol{\sigma}} \cdot \mathbf{v}_{ij}) \hat{\boldsymbol{\sigma}}. \quad (28)$$

Above, $(\mathbf{v}_i, \mathbf{v}_j)$ are the precollisional velocities, $(\mathbf{v}'_i, \mathbf{v}'_j)$ are the postcollisional ones, $\mathbf{v}_{ij} \equiv \mathbf{v}_i - \mathbf{v}_j$ is the relative velocity and $\hat{\boldsymbol{\sigma}}$ is the unit vector pointing from the center of particle j to the center of particle i at the collision. Moreover, in order to simulate the stochastic thermostat, the hard discs are submitted to random kicks every $N_c = 500$ collisions. In the kick, each component of the velocity of every particle is incremented by a random number extracted from a Gaussian distribution of variance $\xi^2 \Delta t$, where Δt is the time interval corresponding to the number of collisions N_c .

In particular, we show the relaxation functions corresponding to $\alpha = 0.3$ ($> \alpha_c$), $\alpha = 0.7$ ($\simeq \alpha_c$), and $\alpha = 0.9$ ($< \alpha_c$)—see panels (a) to (c) of Fig. 2. The symbols represent simulation results from a NESS at $(\xi + \delta\xi)^2 = 0.205$ to the NESS corresponding at $\xi^2 = 0.2$, while the solid lines represent our theoretical prediction (20). The agreement is excellent, which comes as no surprise because the first Sonine approximation is known to give a good description of the granular gas dynamics—although the majority of the studies have been done in the non-linear regime [12, 13, 49].

In principle, Eq. (20) tells us that the relaxation of the granular temperature to the NESS is non-exponential. However, the smallness of the coefficient a_- throughout the whole α range entails that, from a practical point

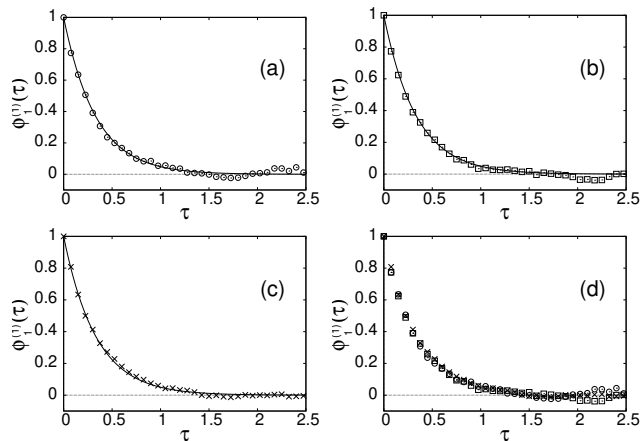


FIG. 2. Relaxation function of the granular temperature as a function of the scaled time τ . Panels (a), (b), and (c) display $\phi_1^{(1)}(\tau)$ for three different values of the restitution coefficient, namely $\alpha = 0.3$, $\alpha = 0.7$ and $\alpha = 0.9$, respectively—symbols correspond to simulation results in a system of 10^6 particles averaged over 10 runs, and lines to the analytical prediction (20). The three simulation curves are plotted together in panel (d), where it is clearly seen that they superimpose. Therefore, the linear relaxation of the granular temperature to the corresponding NESS is “universal” in the τ scale.

of view, the relaxation is very well fitted by a single exponential for all values of the restitution coefficient. Moreover, the relaxation functions for different values of α superimpose, when plotted as a function of the scaled time τ [54]. This is neatly observed in panel (d) of Fig. 2, where we have put together the simulation results from the three previous panels. This stems from the weak α -dependence of the eigenvalue λ_+ , which is close to -3 for all values of α , as predicted by Eq. (24) and shown in panel (a) of Fig. 3. Therein, it is observed that the maximum deviation from -3 is of the order of 3%, for the largest value of a_2^s —i.e. in the completely inelastic limit $\alpha = 0$. For completeness, we show λ_- in panel (b) of the same figure.

Finally, let us consider the evolution of the excess kurtosis in this experiment. Eq. (19) gives, after some algebra, that

$$\phi_2^{(1)}(\tau) = \frac{\delta A_2(\tau)}{\delta\theta(0)} = \frac{a_+ a_- (\lambda_+ - \lambda_-)}{M_{12}} (e^{\lambda_+ \tau} - e^{\lambda_- \tau}). \quad (29)$$

The coefficient in front of the difference of exponentials can also be expanded in powers of a_2^s , making use of Eqs. (9) and (24)–(27), with the result

$$\frac{a_+ a_- (\lambda_+ - \lambda_-)}{M_{12}} = \frac{6}{4B - 3} + \frac{27(5 + 4B)}{8(4B - 3)^3} a_2^s + O(a_2^s)^2. \quad (30)$$

The dominant behaviour $6/(4B - 3)$ is positive for all α : this means that $\delta A_2(\tau)$ has the same sign that $\delta\theta(0)$ for all times, i.e. the same sign of $\delta\xi$ [55]. Note that, in our experiment, the driving is instantaneously decreased

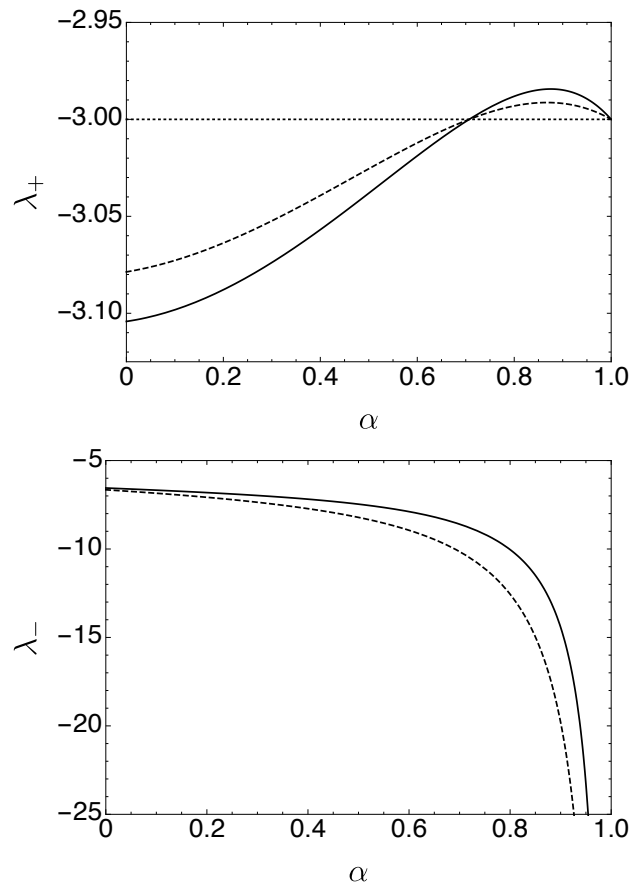


FIG. 3. Relaxation rates λ_{\pm} as a function of the restitution coefficient. Again, both $d = 3$ (solid line) and $d = 2$ (dashed) are plotted. The largest rate λ_+ is always close to -3 throughout. The smaller rate λ_- has a stronger dependence on α , diverging in the elastic limit $\alpha \rightarrow 1^-$.

from $\xi + \delta\xi$ to ξ at the initial time: therefore $\delta\xi > 0$ and $\delta A_2(\tau) > 0$.

Simulation curves for the time evolution of A_2 are compared with the theoretical prediction (29) in Fig. 4. All curves correspond to a system with restitution coefficient $\alpha = 0.3$ and have been averaged over 100 runs. Two experiments in which the driving intensity is decreased from $\xi + \delta\xi$ to ξ are considered. In both cases, we have that $\xi^2 = 0.2$, but with two different values of the jump, $(\xi + \delta\xi)^2 = 0.25$ (squares) and $(\xi + \delta\xi)^2 = 0.35$ (solid circles). Fluctuations in A_2 are larger than those of the granular temperature and thus it is necessary to consider larger jumps in the driving, roughly one order of magnitude larger than those employed in Fig. 2. Still, linear response theory works pretty well: for $(\xi + \delta\xi)^2 = 0.25$, $\delta\xi/\xi \simeq 0.12$ but the agreement is almost perfect; for $(\xi + \delta\xi)^2 = 0.35$, $\Delta\xi/\xi \simeq 0.3$ and the theory only slightly overestimates the relaxation function $\phi_2^{(1)}$. For these larger jumps in the driving, we have also looked into the relaxation of the granular temperature. This is done in Fig. 5, the agreement between the simulation curves and

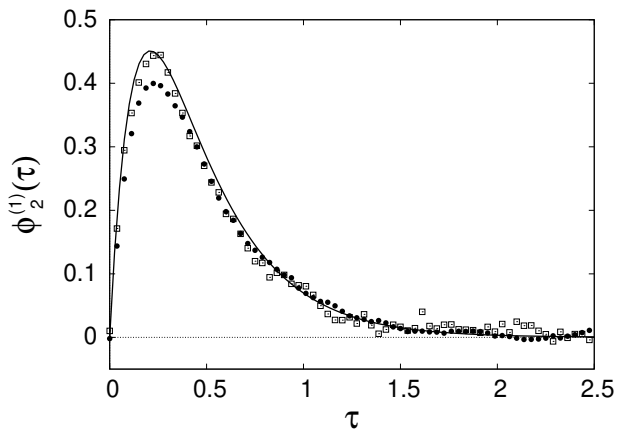


FIG. 4. Relaxation function of the scaled excess kurtosis $A_2 = a_2/a_2^s$ as a function of τ . In the simulations, the driving is instantaneously changed from $(\xi + \delta\xi)^2 = 0.25$ (squares) and $(\xi + \delta\xi)^2 = 0.35$ (solid circles) to $\xi^2 = 0.2$ at $\tau = 0$. Despite the jumps being quite large, the agreement with the theoretical prediction, as given by Eq. (29) (line), is remarkably good.

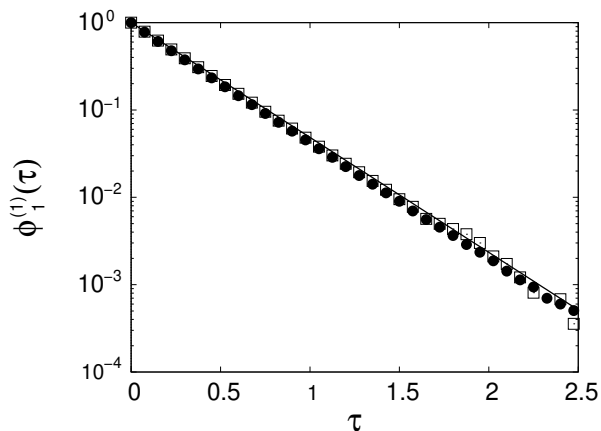


FIG. 5. Relaxation function of the granular temperature for the same situation considered in Fig. 4. Note the logarithmic scale on the vertical axis. Although the jumps in the driving are quite large—relative size of 10–30%, the linear response prediction (solid line) fits perfectly well the simulation results (symbols). The coding for the different lines is the same as in Fig. 4.

the linear response result is even better than that of the excess kurtosis.

IV. THE KOVACS-LIKE EXPERIMENT WITH TWO JUMPS IN THE DRIVING

In this section, we analyse a more complex experiment, which was first done by Kovacs to investigate the glassy response of polymers [34, 35]. The main idea is the following: first, the system under study is “aged” by following a certain protocol. After this aging stage, the sys-

tem has values of its macroscopic variables equal to those in the steady state. However, the macroscopic variables do not remain flat but display a “hump”. This is the Kovacs effect, which tells us that there are other, non-macroscopic, variables that also have to be taken into account to understand the relaxation properties of the system.

Here, we describe the Kovacs-like experiment in terms of the variables of our model [56]. Instead of letting the system relax directly from the NESS for $\xi + \delta\xi$ to that for ξ , at $t = 0$ we suddenly change the driving intensity from $\xi + \delta\xi$ to a lower driving $\xi - \delta\xi' < \xi$. Then, the system starts to relax to the NESS for $\xi - \delta\xi'$, at which $T_s(\xi - \delta\xi') = T_s(\xi) - \delta T' < T_s(\xi)$. At some time—which we call henceforth the waiting time τ_w —the instantaneous value of the granular temperature $T(\tau)$ equals $T_s(\xi)$. At $\tau = \tau_w$, we suddenly change the driving intensity from $\xi - \delta\xi'$ to ξ . This two-jump procedure in the driving characterises the Kovacs protocol.

A qualitative plot of the Kovacs protocol is shown in Fig. 6. Specifically, we have considered the usual case in which $\delta\xi$ and $\delta\xi'$ are both positive and therefore $T_s + \delta T > T_s > T_s - \delta T'$ —sometimes termed the *cooling* protocol. The Kovacs effect is brought to the fore if $T(\tau)$ does not remain flat for $\tau > \tau_w$, signaling that, actually, the system is not in the NESS for the driving intensity ξ after the second jump. If $T(\tau) - T_s > 0$, the Kovacs effect is normal—this is the situation that is always found in molecular systems [34–36], and the one plotted in the figure. If $T(\tau) - T_s < 0$, the Kovacs effect is anomalous, a possibility that has recently been reported in some athermal systems [13, 47, 49].

In the following, we analyse the Kovacs hump in linear response. We employ Eqs. (14) and (15) to write $\delta\theta$ and δA_2 for $\tau \geq \tau_w$, with the change $\tau \rightarrow \tau - \tau_w$ because the initial conditions are given at $\tau = \tau_w$,

$$\delta\theta(\tau_w) = 0, \quad \delta A_2(\tau_w) \neq 0. \quad (31)$$

The coefficients c_{\pm} are proportional to $\delta A_2(\tau_w)$ here, so we have

$$c_{\pm} = \delta A_2(\tau_w) \hat{c}_{\pm}, \quad \hat{c}_+ = -\hat{c}_- = \frac{1}{\lambda_+ - \lambda_-}. \quad (32)$$

Now we introduce a normalised response function for the Kovacs experiment,

$$\begin{aligned} \phi^{(2)}(\tau; \tau_w) &\equiv \frac{\delta z(\tau)}{\delta A_2(\tau_w)} \\ &= \frac{1}{\lambda_+ - \lambda_-} \left(\zeta_+ e^{\lambda_+(\tau - \tau_w)} - \zeta_- e^{\lambda_-(\tau - \tau_w)} \right). \end{aligned} \quad (33)$$

The response of the granular temperature is given by

$$\begin{aligned} \phi_1^{(2)}(\tau; \tau_w) &= \frac{\delta\theta(\tau)}{\delta A_2(\tau_w)} \\ &= \frac{M_{12}}{\lambda_+ - \lambda_-} \left(e^{\lambda_+(\tau - \tau_w)} - e^{\lambda_-(\tau - \tau_w)} \right), \end{aligned} \quad (34)$$

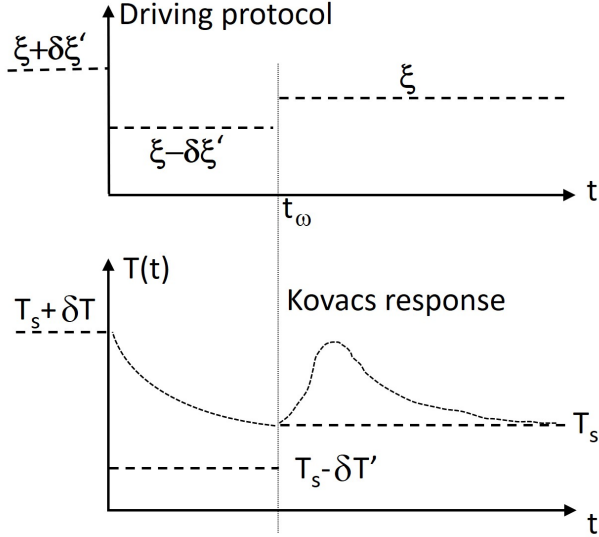


FIG. 6. Qualitative plot of the Kovacs protocol. The system starts from a NESS with granular temperature $T_s + \delta T$, corresponding to a driving $\xi + \delta\xi$. In the waiting time window, the driving is suddenly decreased to $\xi - \delta\xi' < \xi$ and the granular temperature approaches the corresponding steady state value $T_s - \delta T' < T_s$. At the waiting time, the granular temperature equals its steady value for the driving ξ . However, for longer times the granular temperature does not remain flat: it displays a non-monotonic behaviour, the Kovacs hump. The normal case is depicted, in which the temperature displays a maximum, but anomalous behaviour—a minimum instead of a maximum—can also be observed.

whereas that for the excess kurtosis is

$$\phi_2^{(2)}(\tau; \tau_w) = \frac{\delta A_2(\tau)}{\delta A_2(\tau_w)} = a_- e^{\lambda_+(\tau - \tau_w)} + a_+ e^{\lambda_-(\tau - \tau_w)}. \quad (35)$$

On the one hand, the smallness of a_- leads to an almost exponential relaxation for $A_2(\tau)$, with a characteristic time $|\lambda_-|^{-1}$. On the other hand, both modes contribute to the response of the granular temperature, which is non-monotonic.

The value of $\delta A_2(\tau_w)$ is controlled by the relaxation in the waiting time window, in which the driving is equal to $\xi - \delta\xi' < \xi$. Specifically, particularisation of Eq. (29) for $\tau = \tau_w$ yields

$$\delta A_2(\tau_w) = (\delta\theta + \delta\theta') \frac{a_+ a_- (\lambda_+ - \lambda_-)}{M_{12}} (e^{\lambda_+ \tau_w} - e^{\lambda_- \tau_w}) > 0, \quad (36)$$

where we have taken into account that the temperature change in the first jump is $\delta\theta + \delta\theta'$, see Fig. 6. The positivity of $\delta A_2(\tau_w)$ follows from the discussion at the end of Sec. III, just below Eq. (30), and implies that $\delta\theta(\tau)$ and the response function $\phi_1^{(2)}(\tau)$ share the same sign. Therefore, the Kovacs effect is normal (anomalous) when $\phi_1^{(2)}(\tau) > 0$ ($\phi_1^{(2)}(\tau) < 0$).

The definition of the time scale τ , as given by Eq. (4),

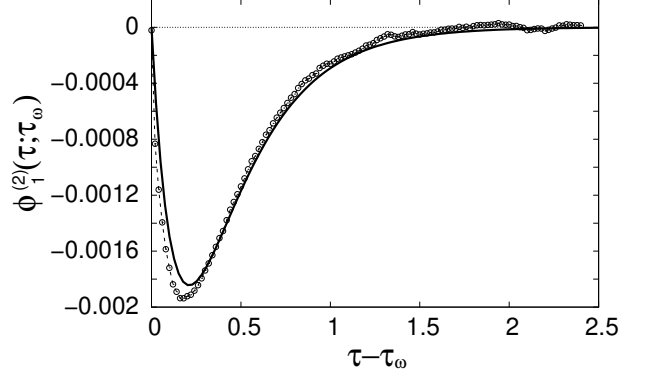


FIG. 7. Kovacs hump for large inelasticity. Specifically, the restitution coefficient is $\alpha = 0.3$. The circles are simulation results obtained with $N = 10^6$ particles averaged over 10^4 runs, while the solid line is our theoretical prediction (34). The Kovacs response is anomalous for this large inelasticity, $\alpha < \alpha_c$.

involves the steady value of the temperature. As a consequence, τ_w on the rhs of Eq. (36) would correspond to the lowest granular temperature $T_s(\xi) - \delta T'$, i.e. that corresponding to the driving $\xi - \delta\xi'$, and not to T_s . However, this difference only impinges on non-linear terms in the jumps. Thus, the scaled waiting time τ_w is calculated with T_s in linear response. Insertion of Eq. (36) into (34) results in

$$\delta\theta(\tau) = (\delta\theta + \delta\theta') a_+ a_- (e^{\lambda_+ \tau_w} - e^{\lambda_- \tau_w}) \times (e^{\lambda_+(\tau - \tau_w)} - e^{\lambda_-(\tau - \tau_w)}). \quad (37)$$

All the terms on the rhs of Eq. (37), except for a_- , are positive definite. As a consequence, it is a_- that controls the sign of the Kovacs response. Normal behaviour, i.e. $\delta\theta(\tau) \geq 0$, is obtained for $a_- > 0$, i.e. for $\alpha > \alpha_c$ —see Eq. (22) and Fig. 1. Anomalous behaviour, i.e. $\delta\theta(\tau) \leq 0$, is obtained for $a_- < 0$, i.e. for $\alpha < \alpha_c$. The situation is thus completely similar to the one found in the non-linear regime [13, 49]: normal behaviour is found for small inelasticity whereas anomalous behaviour comes about for large inelasticity. Anomalous Kovacs response thus persists in the linear response regime, it is not a non-linear effect.

In what follows, we compare simulation results from the DSMC numerical integration of the Boltzmann-Fokker-Planck equation with our theoretical predictions. Specifically, we plot the response function $\phi_1^{(2)}(\tau)$; recall that $\delta\theta$ and $\phi_1^{(2)}$ have the same sign. In order to implement the Kovacs protocol we have taken the following values for the noise intensity: $\xi^2 = 0.2$, $(\xi + \delta\xi)^2 = 0.35$, and $(\xi - \delta\xi)^2 = 0.05$. Fluctuations make these larger jumps necessary to numerically observe the time evolution of the excess kurtosis, which is the quantity bringing about the Kovacs effect. As discussed in Sec. III and il-

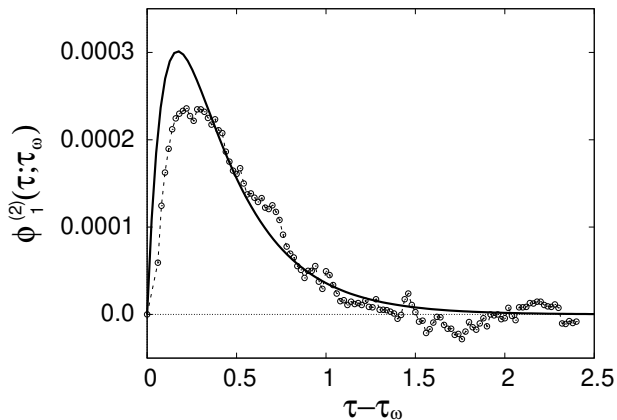


FIG. 8. Kovacs hump for small inelasticity. Specifically, the restitution coefficient is $\alpha = 0.8$. The response is normal in this case, $\alpha > \alpha_c$. The circles are simulation results obtained with $N = 10^6$ particles averaged over 10^4 runs, whereas the solid line is again Eq. (34).

illustrated in Figs. 4 and 5, linear response still holds in this situation. This can be physically understood in this two-jump experiment, because we will see that the size of the memory effect is quite small.

The case $\alpha < \alpha_c$, i.e. the large inelasticity regime, is shown in Fig. 7. Consistently with our theoretical predictions, the Kovacs response is anomalous, $\phi_1^{(2)} < 0$, and the agreement between simulations and theory is excellent. The small inelasticity regime, $\alpha > \alpha_c$ is illustrated in Fig. 8. Here, the response is normal, $\phi_1^{(2)} > 0$. The amplitude of the hump is roughly one order of magnitude smaller than that in Fig. 7. This is the reason why larger fluctuations can be appreciated in the numerical data.

V. DISCUSSION

For small changes of the driving, i.e. in the linear response regime, the relaxation function of the granular

temperature measured in simulations is almost perfectly fitted by a single exponential, over the whole range of inelasticities. In principle, this seems to rule out the possibility of a Kovacs-like effect, since it is well-known that non-exponential relaxation is a prerequisite for the appearance of aging and memory effects—a simple example is the one-dimensional Ising model [16, 19, 20, 44].

Nevertheless, the Kovacs effect is indeed present in the granular gas in linear response: in the Sonine approximation, the relaxation has two modes and thus the relaxation function is not exactly an exponential. The smallness of the coefficient of the second mode makes it very difficult to infer the deviation from the exponential behaviour by looking only at the “experimental” curve. This highlights the difficulty of ruling out the possible emergence of memory effects by investigating only simple, single-jump, relaxation experiments.

An anomalous Kovacs effect has recently been observed in the non-linear regime [13, 47, 49]. We have neatly shown that this anomalous behaviour survives in the linear regime, non-linearities are not necessary to bring it about. Positivity of the coefficients of all the modes in the direct relaxation function entails that the Kovacs effect is necessarily normal in linear response [36, 47, 48]. It is the change of sign of the coefficient of the second mode that gives rise to the anomalous Kovacs effect in linear response. This important feature, which is hardly discernible in the direct relaxation case, is clearly brought to the fore by our analysis of the Kovacs experiment.

The generalisation of the fluctuation-dissipation theorem to non-equilibrium situations makes it possible to relate linear response functions to certain time correlation functions [4]. Therefore, a perspective for future work is the investigation of the emerging time correlation functions in the granular gas. This is a far from trivial task, due to the incomplete knowledge of the steady state distribution. Another possible avenue for future development is the analysis of linear response results in other, more complex, intrinsically non-equilibrium systems, like the rough granular gas [57–59] or active matter [60–65].

-
- [1] R. Kubo, The fluctuation-dissipation theorem, Reports on Progress in Physics **29**, 255 (1966).
 - [2] H. Callen, *Thermodynamics and an Introduction to Thermostatistics* (Wiley, 1985).
 - [3] N. G. Van Kampen, *Stochastic processes in Physics and Chemistry* (North-Holland, 1992).
 - [4] U. M. B. Marconi, A. Puglisi, L. Rondoni, and A. Vulpiani, Fluctuation–dissipation: response theory in statistical physics, Physics Reports **461**, 111 (2008).
 - [5] I. Goldhirsch and G. Zanetti, Clustering instability in dissipative gases, Physical Review Letters **70**, 1619 (1993).
 - [6] J. J. Brey, J. W. Dufty, and A. Santos, Dissipative dynamics for hard spheres, J. Stat. Phys. **87**, 1051 (1997).
 - [7] N. V. Brilliantov and T. Pöschel, *Kinetic Theory of Granular Gases* (OUP Oxford, 2004).
 - [8] A. Puglisi, P. Visco, A. Barrat, E. Trizac, and F. van Wijland, Fluctuations of internal energy flow in a vibrated granular gas, Physical Review Letters **95**, 110202 (2005).
 - [9] T. P. C. Van Noije and M. H. Ernst, Velocity distributions in homogeneous granular fluids: the free and the heated case, Granul. Matter **1**, 57 (1998).
 - [10] J. M. Montanero and A. Santos, Computer simulation of uniformly heated granular fluids, Granular Matter **2**, 53 (2000).
 - [11] A. Santos and J. M. Montanero, The second and third Sonine coefficients of a freely cooling granular gas revisited, Granular Matter **11**, 157 (2009).
 - [12] M. I. García de Soria, P. Maynar, and E. Trizac, Univer-

- sal reference state in a driven homogeneous granular gas, *Physical Review E* **85**, 051301 (2012).
- [13] A. Prados and E. Trizac, Kovacs-Like Memory Effect in Driven Granular Gases, *Physical Review Letters* **112**, 198001 (2014).
- [14] A. Lasanta, F. Vega Reyes, A. Prados, and A. Santos, When the Hotter Cools More Quickly: Mpemba Effect in Granular Fluids, *Physical Review Letters* **119**, 148001 (2017).
- [15] G. W. Scherer, *Relaxation in glass and composites* (Wiley New York, 1986).
- [16] H. Spohn, Stretched exponential decay in a kinetic Ising model with dynamical constraint, *Communications in Mathematical Physics* **125**, 3 (1989).
- [17] W. Kob and R. Schilling, Dynamics of a one-dimensional “glass” model: Ergodicity and nonexponential relaxation, *Physical Review A* **42**, 2191 (1990).
- [18] G. W. Scherer, Theories of relaxation, *J. Non-Cryst. Solids* **123**, 75 (1990).
- [19] J. J. Brey and A. Prados, Stretched exponential decay at intermediate times in the one-dimensional Ising model at low temperatures, *Physica A* **197**, 569 (1993).
- [20] J. J. Brey and A. Prados, Low-temperature relaxation in the one-dimensional Ising model, *Physical Review E* **53**, 458 (1996).
- [21] C. A. Angell, K. L. Ngai, G. B. McKenna, P. F. McMillan, and S. W. Martin, Relaxation in glassforming liquids and amorphous solids, *Journal of Applied Physics* **88**, 3113 (2000).
- [22] J.-P. Bouchaud, Weak ergodicity breaking and aging in disordered systems, *Journal de Physique I* **2**, 1705 (1992).
- [23] L. F. Cugliandolo, J. Kurchan, and F. Ritort, Evidence of aging in spin glass mean-field models, *Physical Review B* **49**, 6331 (1994).
- [24] A. Prados, J. J. Brey, and B. Sánchez-Rey, Aging in the one-dimensional Ising model with Glauber dynamics, *EPL* **40**, 13 (1997).
- [25] C. Josserand, A. V. Tkachenko, D. M. Mueth, and H. M. Jaeger, Memory effects in granular materials, *Physical Review Letters* **85**, 3632 (2000).
- [26] J. J. Brey, A. Prados, M. I. García de Soria, and P. Maynar, Scaling and aging in the homogeneous cooling state of a granular fluid of hard particles, *Journal of Physics A: Mathematical and Theoretical* **40**, 14331 (2007).
- [27] S. R. Ahmad and S. Puri, Velocity distributions and aging in a cooling granular gas, *Physical Review E* **75**, 031302 (2007).
- [28] R. Hecht, S. F. Cieszymski, E. V. Colla, and M. B. Weissman, Aging dynamics in ferroelectric deuterated potassium dihydrogen phosphate, *Physical Review Materials* **1**, 044403 (2017).
- [29] Y. Lahini, O. Gottesman, A. Amir, and S. M. Rubinstein, Nonmonotonic Aging and Memory Retention in Disordered Mechanical Systems, *Physical Review Letters* **118**, 085501 (2017).
- [30] S. Dillavou and S. M. Rubinstein, Nonmonotonic Aging and Memory in a Frictional Interface, *Physical Review Letters* **120**, 224101 (2018).
- [31] E. van Bruggen, E. van der Linden, and M. Habibi, Tailoring relaxation dynamics and mechanical memory of crumpled materials by friction and ductility, *Soft Matter* **15**, 1633 (2019).
- [32] N. C. Keim, J. D. Paulsen, Z. Zeravcic, S. Sastry, and S. R. Nagel, Memory formation in matter, *Reviews of Modern Physics* **91**, 035002 (2019).
- [33] M. Lulli, C.-S. Lee, H.-Y. Deng, C.-T. Yip, and C.-H. Lam, Spatial Heterogeneities in Structural Temperature Cause Kovacs’ Expansion Gap Paradox in Aging of Glasses, *Physical Review Letters* **124**, 095501 (2020).
- [34] A. J. Kovacs, Transition vitreuse dans les polymères amorphes. Etude phénoménologique, *Fortschritte Der Hochpolymeren-Forschung* **3**, 394 (1963).
- [35] A. J. Kovacs, J. J. Aklonis, J. M. Hutchinson, and A. R. Ramos, Isoobaric volume and enthalpy recovery of glasses. II. A transparent multiparameter theory, *Journal of Polymer Science: Polymer Physics Edition* **17**, 1097 (1979).
- [36] A. Prados and J. J. Brey, The Kovacs effect: a master equation analysis, *Journal of Statistical Mechanics: Theory and Experiment*, P02009 (2010).
- [37] A. Buhot, Kovacs effect and fluctuation–dissipation relations in 1d kinetically constrained models, *Journal of Physics A: Mathematical and General* **36**, 12367 (2003).
- [38] E. M. Bertin, J. P. Bouchaud, J. M. Drouffe, and C. Godreche, The Kovacs effect in model glasses, *Journal of Physics A: Mathematical and General* **36**, 10701 (2003).
- [39] J. J. Arenzon and M. Sellitto, Kovacs effect in facilitated spin models of strong and fragile glasses, *The European Physical Journal B-Condensed Matter and Complex Systems* **42**, 543 (2004).
- [40] S. Mossa and F. Sciortino, Crossover (or Kovacs) effect in an aging molecular liquid, *Physical Review Letters* **92**, 045504 (2004).
- [41] G. Aquino, L. Leuzzi, and T. M. Nieuwenhuizen, Kovacs effect in a model for a fragile glass, *Physical Review B* **73**, 094205 (2006).
- [42] G. Diezemann and A. Heuer, Memory effects in the relaxation of the Gaussian trap model, *Physical Review E* **83**, 031505 (2011).
- [43] X. Di, K. Z. Win, G. B. McKenna, T. Narita, F. Lequeux, S. R. Pullela, and Z. Cheng, Signatures of Structural Recovery in Colloidal Glasses, *Physical Review Letters* **106**, 095701 (2011).
- [44] M. Ruiz-García and A. Prados, Kovacs effect in the one-dimensional Ising model: A linear response analysis, *Physical Review E* **89**, 012140 (2014).
- [45] S. Banik and G. B. McKenna, Isochoric structural recovery in molecular glasses and its analog in colloidal glasses, *Physical Review E* **97**, 062601 (2018).
- [46] L. Song, W. Xu, J. Huo, F. Li, L.-M. Wang, M. D. Ediger, and J.-Q. Wang, Activation Entropy as a Key Factor Controlling the Memory Effect in Glasses, *Physical Review Letters* **125**, 135501 (2020).
- [47] R. Kürsten, V. Sushkov, and T. Ihle, Giant Kovacs-Like Memory Effect for Active Particles, *Physical Review Letters* **119**, 188001 (2017).
- [48] C. A. Plata and A. Prados, Kovacs-Like Memory Effect in Athermal Systems: Linear Response Analysis, *Entropy* **19**, 539 (2017).
- [49] E. Trizac and A. Prados, Memory effect in uniformly heated granular gases, *Physical Review E* **90**, 012204 (2014).
- [50] A. Lasanta, F. V. Reyes, A. Prados, and A. Santos, On the emergence of large and complex memory effects in nonequilibrium fluids, *New Journal of Physics* **21**, 033042 (2019).
- [51] This expression for B stems from a lengthy kinetic theory calculation [12] or, preferably, from a simple self-consistency argument [13, 49].

- [52] They are non-linear in the temperature but linear in the excess kurtosis. This is a consequence of the first Sonine approximation, in which non-linearities in a_2 are neglected.
- [53] We are employing a notation similar to that introduced in Ref. [48] to investigate the linear response of a general athermal system, at the level of description of the equations for the moments.
- [54] They do not superimpose as a function of the real time t . The definition of the scaled time in Eq. (4) involves α because the parameter ζ_0 is proportional to $1 - \alpha^2$. Therefore, the smaller the inelasticity $1 - \alpha$ is, the slower the relaxation in real time becomes.
- [55] The steady value of the granular temperature is an increasing function of the driving, both $\delta\theta(0)$ and $\delta\xi$ have the same sign.
- [56] Aside from the original papers by Kovacs [34, 35], the account of the original experiment can be found in many places, see for example Refs. [15, 18, 36].
- [57] G. M. Kremer, A. Santos, and V. Garzó, Transport coefficients of a granular gas of inelastic rough hard spheres, *Physical Review E* **90**, 022205 (2014).
- [58] F. V. Reyes, A. Santos, and G. M. Kremer, Role of roughness on the hydrodynamic homogeneous base state of inelastic spheres, *Physical Review E* **89**, 020202 (2014).
- [59] A. Torrente, M. A. López-Castaño, A. Lasanta, F. V. Reyes, A. Prados, and A. Santos, Large Mpemba-like effect in a gas of inelastic rough hard spheres, *Physical Review E* **99**, 060901 (2019).
- [60] A. Baskaran and M. C. Marchetti, Enhanced Diffusion and Ordering of Self-Propelled Rods, *Physical Review Letters* **101**, 268101 (2008).
- [61] A. Baskaran and M. Cristina Marchetti, Nonequilibrium statistical mechanics of self-propelled hard rods, *Journal of Statistical Mechanics: Theory and Experiment* , P04019 (2010).
- [62] T. Ihle, Kinetic theory of flocking: Derivation of hydrodynamic equations, *Physical Review E* **83**, 030901 (2011).
- [63] M. C. Marchetti, J. F. Joanny, S. Ramaswamy, T. B. Liverpool, J. Prost, M. Rao, and R. A. Simha, Hydrodynamics of soft active matter, *Reviews of Modern Physics* **85**, 1143 (2013).
- [64] T. Ihle, Chapman–Enskog expansion for the Vicsek model of self-propelled particles, *Journal of Statistical Mechanics: Theory and Experiment* , 083205 (2016).
- [65] L. L. Bonilla and C. Trenado, Contrarian compulsions produce exotic time-dependent flocking of active particles, *Physical Review E* **99**, 012612 (2019).